

## 1.1 A Program for Optimizing SRF Linac Costs

Tom Powers

Mail to: [powers@jlab.org](mailto:powers@jlab.org)

Thomas Jefferson National Accelerator Facility, Newport News, VA

### 1.1.1 Introduction

Every well-designed machine goes through the process of cost optimization several times during its design, production and operation. The initial optimizations are done during the early proposal stage of the project when none of the systems have been engineered. When a superconducting radio frequency (SRF) linac is implemented as part of the design, it is often a difficult decision as to the frequency and gradient that will be used. Frequently, such choices are made based on existing designs, which invariably necessitate moderate to substantial modifications so that they can be used in the new accelerator. Thus the fallacy of using existing designs is that they will frequently provide a higher cost machine or a machine with sub-optimal beam physics parameters. This paper describes preliminary results of a new software tool that allows one to vary parameters and understand the effects on the optimized costs of construction plus 10 year operations of an SRF linac, the associated cryogenic facility, and controls, where operations includes the cost of the electrical utilities but not the labor or other costs. It derives from collaborative work done with staff from Accelerator Science and Technology Centre, Daresbury, UK [1] several years ago while they were in the process of developing a conceptual design for the New Light Source project. The initial goal was to convert a spread sheet format to a graphical interface to allow the ability to sweep different parameter sets. The tools also allow one to compare the cost of the different facets of the machine design and operations so as to better understand the tradeoffs.

### 1.1.2 Software Description

#### 1.1.2.1 *General structure*

The program was written in LabView in a state machine format. This allows one to separate, and/or modify the different subroutines, jump to different states, add different parameters, and/or expand the program to include different aspects of machine design. The input variables are contained in clusters of variables, one for the cavity/cryomodule parameters, one for the system cost parameters and one for the cryogenic heat loads. There is a cluster for the program outputs such as cost and design points.

Authored by Jefferson Science Associates, LLC under U.S. DOE Contract No. DE-AC05-06OR23177. The U.S. Government retains a non-exclusive, paid-up, irrevocable, world-wide license to publish or reproduce this manuscript for U.S. Government purposes.

### 1.1.2.2 *Input / Output Parameters*

The program has two loss parameters for cryogenic losses. Static losses of each of the SRF cryo-assembly, called a cryomodule, and RF driven, or dynamic, losses. The static heat losses include the cryomodule, associated valve box, and per kilometer transfer line losses. A detailed list of the current input output parameters is given in Table 1. Figure 1 shows the user interface for modifying variables in the program while Figure 2 shows the graphical output that is available. At any given point in time all parameters for a swept variable run can be output to a tab delimited text file.

**Table 1:** Input/output parameter list.

<b>SRF Parameters</b>	<b>Baseline Costs</b>	<b>Outputs</b>
Final Linac Energy (GeV)	Cryomodule Cost (\$M/unit)	Total (\$M)
Gradient (V/m)	RF Power (\$/W)	Construction (\$M)
Frequency (Hz)	RF Control, etc. (\$k/Cavity)	Cryogenic Plant (\$M)
Cavities Per Cryomodule	Inter CM Girder (\$k/unit) <sup>3</sup>	Cryomodules (\$M)
Active Length Per Cavity (m)	Tunnel Civil (\$k/m)	Girders (\$M)
Packing Factor Tot L/Active L	AC Power (\$/MW-Hour)	Tunnel, etc. Civil (\$M)
Normalized Shunt Imp. ( $\Omega$ /m)	5kW @ 2K Plant (\$M)	10 Year Power (\$M)
$B_{PEAK}/E_{ACC}$ (mT/(MV/m))	5kW Plant Civil (\$M)	Linac Length (m)
Geometry Factor ( $\Omega$ )	Transfer Line (\$k/m)	Num. Cryomodules
Beam Current (A)	2K Plant Margin	Num. Cavities
Beam Phase (deg)	% Increase Plant Cost @ 1.8K	Num. Girders, etc.
Detune Frequency Budget (Hz)	% Decrease in Eff. @ 1.8K	CM Dynamic Heat (W)
RF Power Margin	Linac R&D Cost (\$M)	Linac 2K Heat (W)
Operating Temperature (K)	RF Wall Plug Eff.	2K With Margin
Maximum Loaded-Q	Controls AC Pwr / Girder (kW)	$Q_0$
Loaded-Q Uncertainty	Operations Week	Matched $Q_L$
Material and Treatment <sup>1</sup>	Power Overhead <sup>4</sup>	RF Power Per Cavity (kW)
Beam Transient Handling <sup>2</sup>	Static Heat Load/CM (W) <sup>5</sup>	Cryo AC Power (MW)
	Transfer Line Heat (W/km)	Non-Cryo AC Power (MW)

Notes:

1. A combination of materials and treatments were modeled in the  $Q_0$  calculations. These were permutations of fine grain niobium and large grain niobium and vacuum baked at 120°C or not vacuum baked at 120°C.
2. The phase of the beam current can have a substantial impact on optimizing the loaded-Q and RF power requirements in an SRF Cavity.[2] Under certain circumstances the RF power requirements are substantially higher for short periods of time. There are techniques which can be used to compensate for said transients, such as slowly ramping up the beam current while the cavity tuners operate.
3. The inner cryomodule girder is the vacuum hardware, beam diagnostics hardware, and magnets that make up the common beam line hardware set between cryomodules. Also included in this item are the controls electronics and magnet power supplies.
4. The Power overhead in the baseline costs column includes items such as lighting, HVAC, and cooling tower power. An increase of 25% over the calculated electrical demand was used for this parameter.

5. The static heat load per cryomodule included the losses in the cryomodule as well as the associated valve boxes.

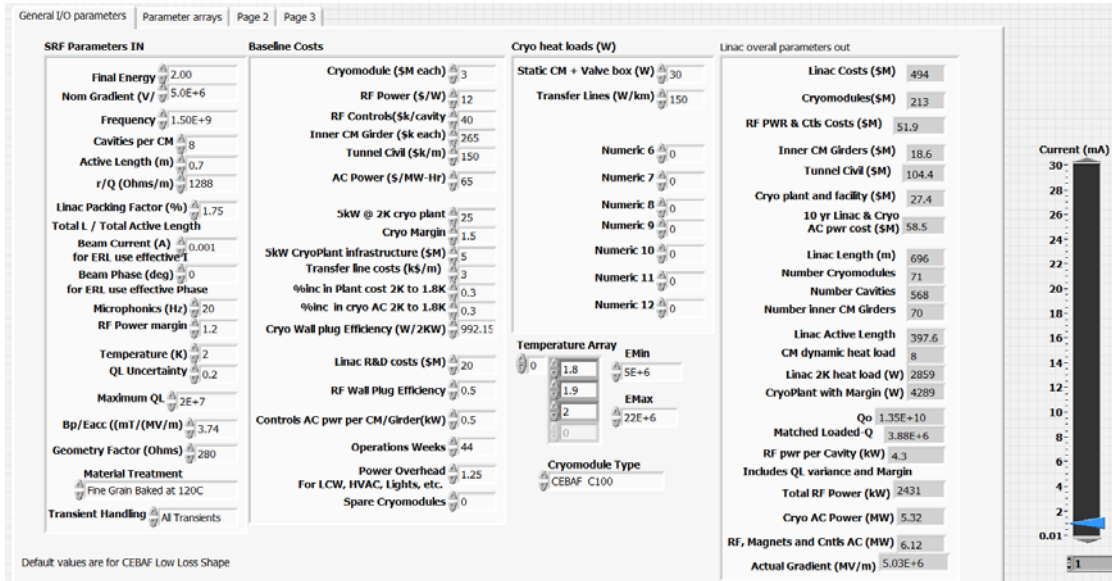


Figure 1: Input / Output screen of optimization program.

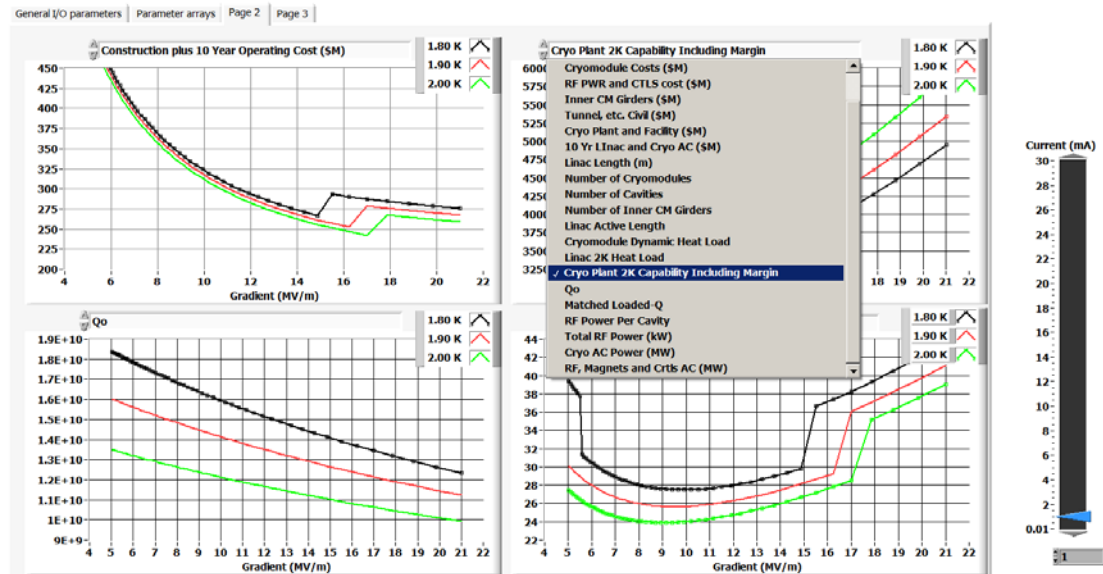
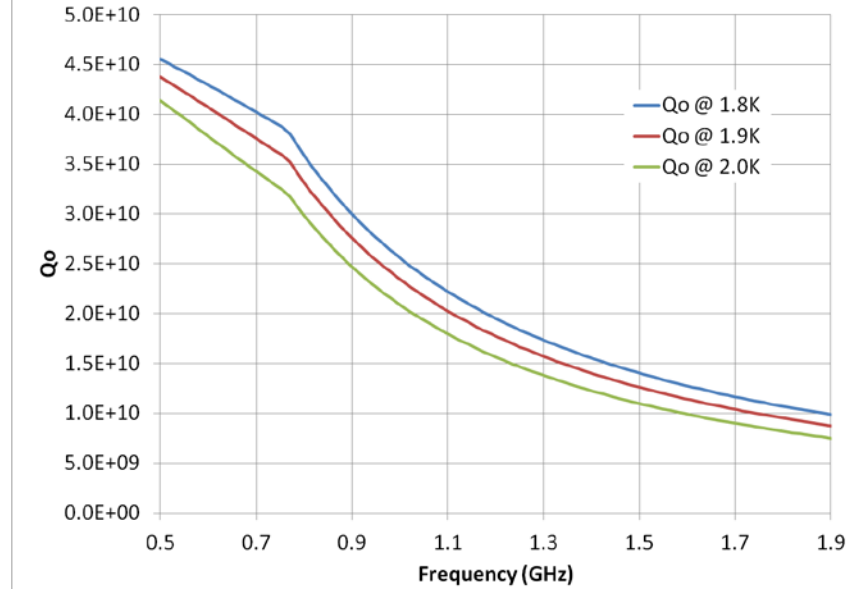


Figure 2: Graphics screen of optimization program showing method for selecting data to plot.

### 1.1.2.1 Calculating $Q_0$

$Q_0$  is calculated for each data point, and is based on a compilation of historic data. This historical data is a compilation from measurements taken in the vertical test area at Jefferson Lab, where, over the past 20 years JLAB staff has performed more than 1800 tests on superconducting cavities of various configurations and frequencies. A series of curve fits were done on these data in order to determine a  $Q_0$  value as a function of gradient, frequency and operating temperature.[3] The analysis was limited in a number of areas due to a lack of completed data sets. It does take into account low to mid field

Q-slope as well as the basic material parameters, cavity shapes, etc. It does not take into account high field slope which is an area that is currently undergoing revision. Another area that is under review is  $Q_0$  degradation between vertical test and cryomodule installation in the accelerator, as well as long term degradation of the  $Q_0$  in operational conditions. Figure 3, shows the value of  $Q_0$  as a function of frequency at 16 MV/m at three different temperatures. For this data the cavity models used had the same geometry factor, and ratio of peak magnetic field to average electric field as the CEBAF low loss cavities used in the 12 GeV upgrade.



**Figure 3:**  $Q_0$  as a function of frequency and temperature at 16 MV/m. All frequencies scaled from CEBAF C100 upgrade cavity.

#### 1.1.2.2 Calculating Loaded-Q and RF Power

The matched loaded-Q is the loaded-Q such that the installed RF power is minimized. As discussed in the *Input/Output Parameters* section, the selected loaded-Q values depend on whether the RF power can maintain gradient regulation under all transient beam loading conditions or only in a steady state condition. Eq. (1) provides the matched loaded-Q value under all transient conditions, while Eq. (2) gives the matched loaded-Q value under steady state conditions.

$$Q_L|_{MinPower} = \frac{E}{\sqrt{(I_0(r/Q)\cos\psi_B)^2 + \left(\pm 2\frac{\delta f}{f_0}E + I_0(r/Q)\sin\psi_B\right)^2}} \quad (1)$$

$$Q_L|_{MinPower} = \frac{E}{\sqrt{(I_0(r/Q)\cos\psi_B)^2 + \left(2\frac{\delta f}{f_0}E\right)^2}} \quad (2)$$

Here,  $E$  is the gradient in V/m,  $I_0$  is the effective beam current in amperes,  $(r/Q)$  is the normalized shunt impedance in Ohms/m,  $\psi_B$  is the phase of the beam current relative to the cavity gradient,  $\delta f$  is the difference between the RF frequency and  $f_0$  which is the resonant frequency of the cavity.[4]

Once the matched loaded-Q is determined, it is used along with the detune frequency budget, the uncertainty in the loaded-Q and the remainder of the cavity parameters to calculate the permutations on the forward power necessary for operation at each point. The maximum value of this data set is used as the minimum RF power required. This is multiplied by the RF power margin to determine the RF power per cavity. There is no margin in the RF power for cavities operated above the design value, which is an area for future modifications to the program.

#### 1.1.2.1 Cryogenic Facility Costs

Figure 4 shows the cost and efficiency estimates used for the cryogenic plant as a function of “2 K” power. The baseline plant and infrastructure costs that were used were that of the 5 kW at 2 K plant that was built as part of the CEBAF 12 GeV upgrade.[5] One major assumption is that the ratio of 50 K shield power to 2 K power is similar to that in CEBAF. Another critical aspect of the actual costs is that the plant was designed by, major components procured by, and the system integrated by JLAB staff. Were the plant to be procured as a turn-key plant the costs would likely be significantly higher. The procurement, installation and commissioning costs are scaled as the ratio of the  $(2 \text{ K power}/5 \text{ kW})^{0.7}$ . [5] The wall plug efficiency, being the ratio of the total AC power divided by the 2 K power, was determined by plotting the efficiency achieved by several existing plants used at accelerators [6] and generating a third order fit between 800 W and 5 kW at 2K. It includes all AC power including warm compressors. Cooling towers, HVAC, lighting, etc. are included as part of a separate line item based on the overall power budget. The plant cost and efficiency was increased linearly by 30% between 2 K and 1.8 K. [5].

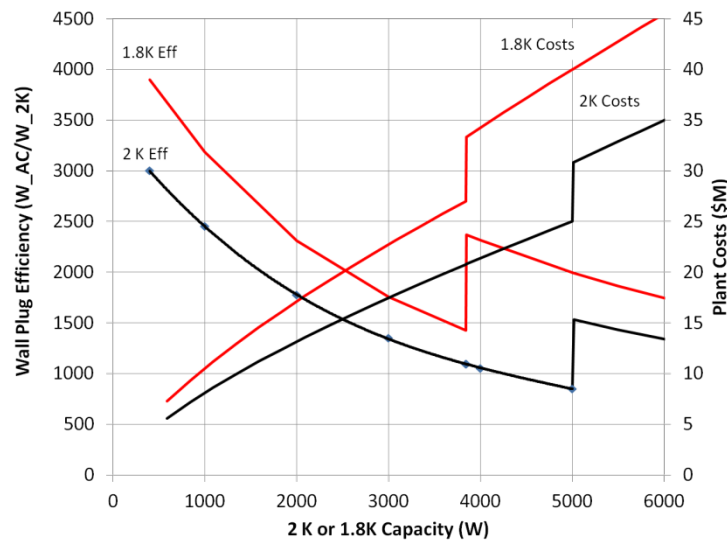


**Figure 4:** The wall plug efficiency and facility plant procurement costs for a helium refrigerator operated at 2.0 K and 1.8 K respectively.

The steps at 5 kW and 3.8 kW for the 2 K and 1.8 K systems were based on the practical aspect of building and shipping the components.[5] The primary issue is shipping of an assembled cold box by truck. Above these power break points the plant must be split into two sections. While one might consider using plants of different power ratings in order to reduce the cost, such plants might be less than ideal when

considering standby (half power) operations, spare parts, engineering design costs, and overall maintenance costs. Based on this the model simply divides the plant into two equal sized plants. The efficiency steps up to match that of the smaller plant.

### 1.1.3 Results

#### 1.1.3.1 *Cost as a function of frequency*

One approach to the analysis of cost as a function of frequency is to maintain a constant active length of the linac. Figure 5 shows such an analysis where a 2 GeV linac was modeled with 21 cryomodules and a linac total active length of 118 m. In this model, as is often done when performing this type of optimization, cavities are not causal as it relies on a fractional number of cavities per cryomodule. Alternately one could consider using an integer number of cavities per cryomodule, which would limit the model to approximately 10 points for the same parameter sweep.

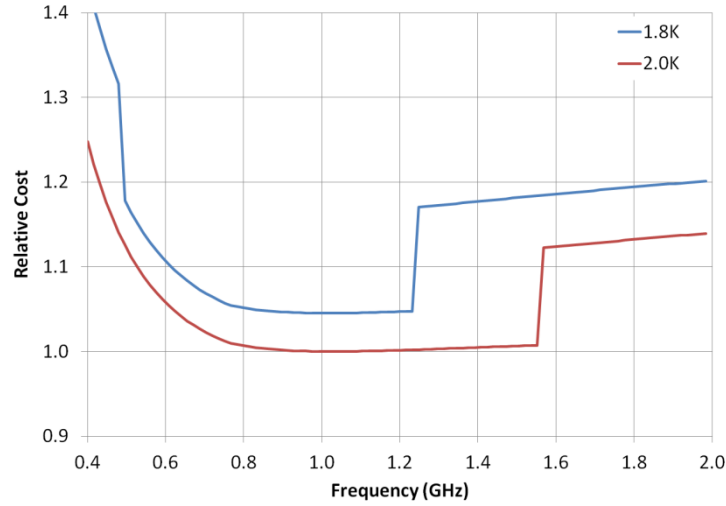


**Figure 5:** Relative cost of a 118 m active length, 21 cryomodule, 2 GeV linac plus 10 years of electrical power as a function of frequency and temperature.

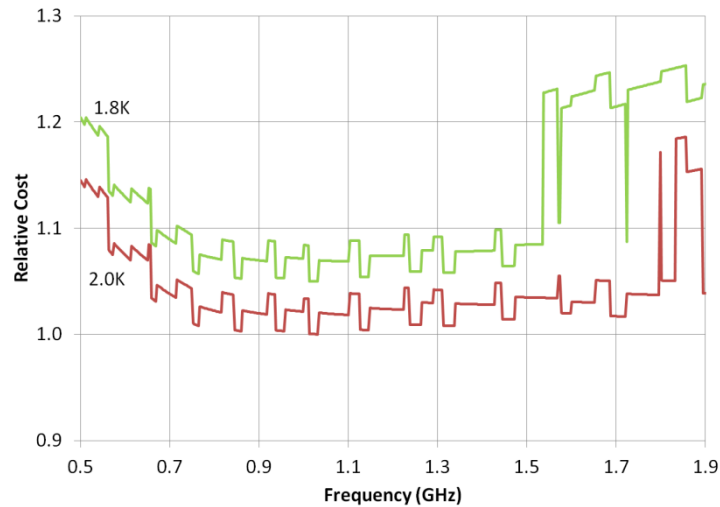


**Figure 6:** Relative cost of a 2 GeV linac plus 10 years of electrical power as a function of frequency and temperature for 10 – 12 m cryomodules each with a maximum of 8m of active length and an integer number of cavities.

Alternately, one can use practical cryomodules. For the results shown in Figure 6, the cryomodules were limited to 8 m of active length, resulting in 10 m to 12 m cryomodule lengths. The number of cells per cavity was varied from 4 cells at 500 MHz up to 11 cells above 1800 MHz resulting in cavities that are less than 1.2 m active length for any given cavity. This results in quantized steps in the relative costs plots. In these results, the steps are changes in the number of cryomodules. Also as one changes the frequency for a given cryomodule configuration the gradient must be reduced slightly (up to 10%) so as to provide the target machine energy. At lower frequencies the model for  $Q_0$  currently employed does not have gradient dependence and thus there is a downward slope in the overall costs (lower cryogenic needs at lower gradients). At higher frequencies the  $Q_0$  slope more than makes up for the reduction in gradient and the  $Q_0$  losses increase as a function of frequency.

#### 1.1.3.1 Cost as a function of gradient

For this model the program was set up with fixed cryomodule and cavity parameters and by sweeping the gradient, one is able to better understand the cost drivers and implications. In actuality the program is sweeping through the number of cryomodules and calculating the average gradient such that the desired energy is achieved. Note that if the machine is run off crest, for a given number of cryomodules the gradient will have to be increased by a factor of  $1/\cos(\psi_B)$  in order to provide the design beam energy gain. Figure 7 shows the relative cost of the C100 cryomodule design which was used in the 12 GeV upgrade.[7] The C100 cryomodule contains 8 cavities, each with seven cells operated at 1497 MHz, where each of the cavities has a normalized shunt impedance of  $1288 \Omega/\text{m}$  and a geometry factor of  $280 \Omega$ . This was compared to a cryomodule that could be built out of 6 cavities, of 5 cells each operated at 748.5 MHz. For this model the cavities had a normalized shunt impedance of  $644 \Omega/\text{m}$  and a geometry factor of  $280 \Omega$ .

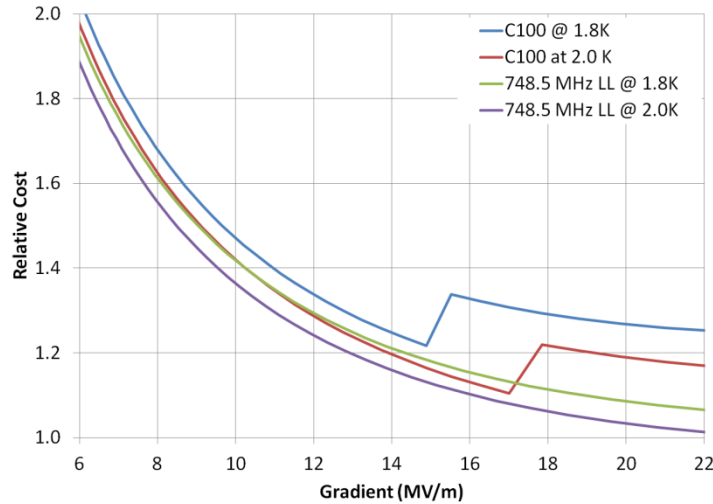


**Figure 7:** Relative cost of a 2 GeV linac plus 10 years of electrical power as a function of gradient and temperature.

Figure 8 shows the relative cost breakdown for the same C100 cryomodule configuration. One can see that the cost driver at the lower gradients is the cryomodule and accelerator civil construction costs. At higher gradients there is a step increase in



cryogenic costs as the system exceeds a 5 kW or 3.8 kW cryogenic plant rating for 2.0 K and 1.8 K operating points respectively.

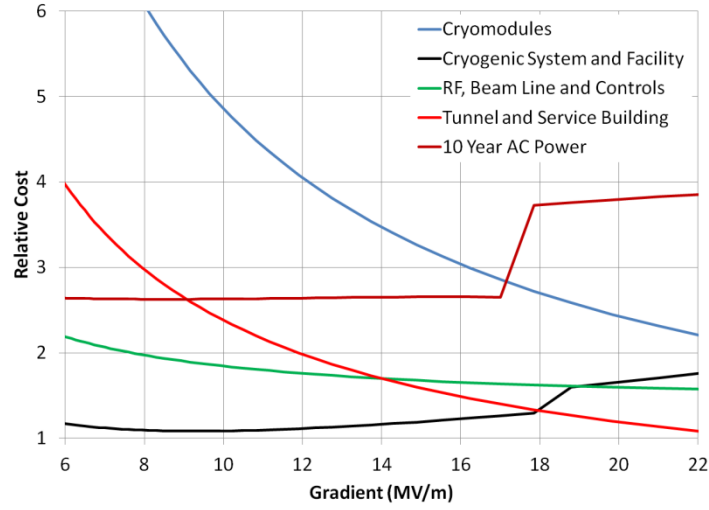


**Figure 8:** Relative cost breakdown for the components used in determining the cost for the C100 cryomodule operated at 2.0 K.

#### 1.1.4 Model Deficiencies and Future Improvements.

The model used for the results in this paper has a number of issues which still need to be addressed. The cost estimates for items such as inner cryomodule girders, cryomodules, RF power, RF control, construction costs, etc. need to be estimated on a machine by machine, and location by location basis. Also since the current model uses a fixed number for the cryomodule unit cost, it is important to note that cryomodules with different numbers of cavities, couplers, etc. have different costs. In addition to issues like coupler selection, etc. the program does not take into account the material costs increases that occur when building cryomodules at lower frequencies.

The  $Q_0$  data used for the analysis was taken from vertical tests. Thus there is no accounting for degradations and additional RF losses due to phenomena such as imperfect magnetic shielding, fundamental power coupler losses, and long term degradation due to new field emitters all of which occur when the cavities are installed and operated in a cryomodule. The model does not include high field  $Q$ -slope or any distribution function for field emission losses. Further analysis of state of art production data as well as data from past production runs and data from operational machines should allow us to refine the  $Q_0$  models used. Reviewing actual costs for specific systems, hardware and constructions, as well as those included in proposals for new machines should provide us with results that are more in line with reality. In addition to addressing these issues we would like to also include more accurate distributions of gradients into the model which will affect the cryogenic losses.

#### 1.1.5 Conclusions

These tools allow one to better understand the tradeoffs relating to the top level design parameters of an SRF linac. They allow one to make adjustments to the baseline costs, cavity parameters, machine packing factors, etc. on the fly and to get a quick feedback as to the impact. One surprise to the author was the major cost implications



that occur when one exceeds the 18 kW at 4K helium liquefier limitations. Since this describes initial applications of a new program, any use of the results of the simulation in its current state should be done with care. For example, simple things such as inclusion of field emission onset, or Q-slope changes at lower frequencies, can dramatically change the optimum operations frequency, as both would tend to degrade high field operations. Inclusion of high field Q-slope will lead to increases in costs at the higher field levels and may lead to lower optimized field. Additionally, although the baseline cost information is felt to be reasonable, different locations will have different construction and electric power costs. Although we have made good progress in developing the tools for understanding machine cost tradeoffs more work is necessary in order to understand all of the impacts of the different parameters.

### 1.1.6 References

1. McIntosh, P., Accelerator Science and Technology Centre, Daresbury, UK, personal communication, May 2009.
2. Powers, T., "RF Controls Experience with the JLAB IR Upgrade FEL," 2009 ERL Workshop, Ithaca, NY, June, 2009.
3. Ciovati, G., et. al., "Residual Resistance Data from Cavity Production Projects at Jefferson Lab," IEEE Transactions on Applied Superconductivity, Vol 21, No. 3, June 2011.
4. Powers, T., "Practical Aspects of SRF Cavity Testing and Operations," Tutorial, SRF Workshop, Chicago, IL, July 2011.
5. Arenius, D., Thomas Jefferson National Accelerator Facility, Newport News, VA, personal communications, Feb. 2013.
6. Ganni, R., et. al., "Cryogenic Systems Improvements," Presented at The Thomas Jefferson National Accelerator Science and Technology Review, May, 2008.
7. Pilat, F., "JLAB Upgrade," Presented at Linac 12, Tel Aviv, Israel, Sept. 2012.